J|A|C|S ARTICLES

Published on Web 12/22/2009

Plasmon-Induced Photodegradation of Toxic Pollutants with Ag−AgI/Al_2O_3 under Visible-Light Irradiation

Chun Hu,* Tianwei Peng, Xuexiang Hu, Yulun Nie, Xuefeng Zhou, Jiuhui Qu, and Hong He

State Key Laboratory of Environmental Aquatic Chemistry, Research Center for Eco-Environmental Sciences, Chinese Academy of Sciences, Beijing 100085, China

Received May 16, 2009; E-mail: huchun@rcees.ac.cn

Abstract: A plasmonic photocatalyst Ag−AgI supported on mesoporous alumina (Ag−AgI/Al_2O_3) was prepared by deposition−precipitation and photoreduction methods. The catalyst showed high and stable photocatalytic activity for the degradation and mineralization of toxic persistent organic pollutants, as demonstrated with 2-chlorophenol (2-CP), 2,4-dichlorophenol (2,4-DCP), and trichlorophenol (TCP) under visible light or simulated solar light irradiation. On the basis of electron spin resonance, cyclic voltammetry analyses under a variety of experimental conditions, two electron transfer processes were verified from the excited Ag NPs to AgI and from 2-CP to the Ag NPs, and the main active species of $O_2^{\bullet-}$ and excited h^+ on Ag NPs were involved in the photoreaction system of Ag−AgI/Al_2O_3. A plasmon-induced photocatalytic mechanism was proposed. Accordingly, the plasmon-induced electron transfer processes elucidated the photostability of Ag−AgI/Al_2O_3. This finding indicates that the high photosensitivity of noble metal NPs due to surface plasmon resonance could be applied toward the development of new plasmonic visible-light-sensitive photocatalysts and photovoltaic fuel cells.

Introduction

Heterogeneous photocatalysis has been considered as a cost-effective alternative for the destruction of persistent toxic organic compounds.[1,2] One obstacle to its practical application is the inefficient use of solar energy. The development of visible-light photocatalysts has become one of the most important topics in the photocatalysis field. A variety of preparation methods are used to synthesize visible-light-induced photocatalysts such as ion-injection,[3] mechanochemical synthesis,[4] solvothermal synthesis,[5] and plasma treatment method.[6] There are two approaches to exploit the photocatalysts responsive to visible light: the first involved the substitutional doping of metals and nonmetals for some UV-active oxide, such as TiO_2[7−12] and $InTaO_4$[13] to turn visible photocatalysts. The second is the composite metal oxides visible photocatalysts, such as $PbBi_2Nb_2O_9$,[14] Bi_2WO_6,[15] and $CaFe_2O_4/PbBi_2Nb_{1.9}W_{0.1}O_9$.[16] However, these photocatalysts still could not be applied for the practical solar purification due to low activities and stability. New and more efficient visible-light photocatalysts are needed to meet the requirements of future environmental and energy technologies driven by solar energy. Noble metal nanoparticles (NPs) exhibit strong UV−vis absorption due to their plasmon resonance, which is produced by the collective oscillations of surface electrons.[17,18] Tian and Tatsuma[19] studied plasmon-induced photoelectrochemistry in gold−titanium dioxide (Au−TiO_2) films in the visible-light region. A simultaneous, two electron transfer process occurred from the photoexcited Au NPs to the TiO_2 conduction band and from a solution donor to the Au particle. The photosensitivity of these noble metallic NPs is potentially applicable to the development of a new class of plasmonic photocatalysts and photovoltaic fuel cells. Several plasmonic photocatalysts were developed for photocatalytic decolorization of dyes.[20,21] Despite these promising studies, photoinduced catalytic mechanism and the stability of noble metallic NPs during the photocatalytic

(1) Hoffmann, M. R.; Martin, S. T.; Choi, W.; Bahnemann, D. W. *Chem. Rev.* **1995**, *95*, 69–96.
(2) Martin, H. M. *Photodegradation of Water Pollutants*; CRC Press: Boca Raton, FL, 1996.
(3) Anpo, M.; Ichihashi, Y.; Takeuchi, M.; Yamashita, H. *Res. Chem. Intermed.* **1998**, *24*, 143–149.
(4) Yin, S.; Zhang, Q.; Saito, F.; Sato, T. *Chem. Lett.* **2003**, *32*, 358–359.
(5) Yin, S.; Aita, Y.; Komatsu, M.; Wang, J.; Tang, Q.; Sato, T. *J. Mater. Chem.* **2005**, *15*, 674–682.
(6) Ihara, T.; Miyoshi, M.; Ando, M.; Sugihara, S.; Iriyama, Y. *J. Mater. Chem.* **2001**, *36*, 4201–4207.
(7) Yamashita, H.; Harada, H.; Misaka, J.; Takeuchi, M.; Ikeue, K.; Anpo, M. *J. Photochem. Photobiol., A* **2002**, *148*, 257–261.
(8) Asahi, R.; Morikawa, T.; Ohwaki, T.; Aoki, K.; Tao, Y. *Science* **2001**, *293*, 269–271.
(9) Morikawa, T.; Ohwaki, T.; Suzuki, K.; Moribe, S.; Tero-Kubota, S. *Appl. Catal., B* **2008**, *83*, 56–62.
(10) Yin, S.; Liu, B.; Zhang, P.; Morikawa, T.; Yamanaka, K.; Sato, T. *J. Phys. Chem. C* **2008**, *112*, 12425–12431.
(11) Khan, S. U. M.; Al-Shahry, M.; Ingler, W. B., Jr. *Science* **2002**, *297*, 2243–2245.
(12) Sakthivel, S.; Kisch, H. *Angew. Chem., Int. Ed.* **2003**, *42*, 4908–4911.
(13) Zou, Z.; Ye, J.; Sayama, K.; Arakawa, H. *Nature* **2001**, *424*, 625–627.
(14) Kim, H. G.; Hwang, D. W.; Lee, J. S. *J. Am. Chem. Soc.* **2004**, *126*, 8912–8913.
(15) Amano, F.; Yamakata, A.; Nogami, K.; Osawa, M.; Ohtani, B. *J. Am. Chem. Soc.* **2008**, *130*, 17650–17651.
(16) Kim, H. G.; Borse, P. H.; Choi, W.; Lee, J. S. *Angew. Chem., Int. Ed.* **2005**, *44*, 4585–4589.
(17) Jin, R.; Cao, Y. C.; Mirkin, C. A.; Kelly, K. L.; Schatzand, G. C.; Zheng, J. G. *Science* **2001**, *294*, 1901–1903.
(18) Link, S.; El-Sayed, M. A. *J. Phys. Chem. B* **1999**, *103*, 8410–8426.
(19) Tian, Y.; Tatsuma, T. *J. Am. Chem. Soc.* **2005**, *127*, 7632–7637.

degradation have not, to our knowledge, been reported. In addition, no direct evidence exists providing a clear reaction mechanism for plasmon-induced photodegradation of pollutants. An in-depth understanding of the above issues is essential to devise practical solutions so that this technology can be employed to eliminate a wide variety of pollutants.

Ag halides are well-known photosensitive materials that are widely employed as source materials in photographic films. However, their photocatalytic activity has not been addressed due to labile photodecomposition. Several studies have shown that supported Ag halides exhibit higher photocatalytic activity and photostability.[22−24] This may be attributable to the plasmon resonance of Ag NPs formed on the surface of Ag halide particles.[19] Nevertheless, the exact mechanism of this enhanced photostability has not yet been elucidated.

A plasmonic photocatalyst is described herein consisting of Ag NPs−Ag iodide (AgI) supported on mesoporous alumina ($Ag-AgI/Al_2O_3$) using the deposition−precipitation and photoreduction method. Organic compounds, especially phenolic compounds, are considered to be hazardous wastes, which are highly toxic and difficult to degrade biologically, leading to a setting up of rigid limits on the acceptable level of phenol in the environment. Several ubiquitous water pollutant phenolic compounds, 2-chlorophenol (2-CP), 2,4-dichlorophenol (2,4-DCP), and trichlorophenol (TCP), were selected to evaluate the activity and properties of the catalysts under visible-light irradiation. The photocatalytic activity of AgI/Al_2O_3 is greatly enhanced as it is further loaded with Ag NPs under visible irradiation for the degradation and mineralization of the tested phenolic compounds. A plasmon-induced photocatalytic mechanism was verified by electron spin resonance (ESR) and cyclic voltammetry (CV) analyses under a variety of experimental conditions. Accordingly, the charge transfer processes, including from the plasmon-excited silver to AgI and pollutants to the silver, evidenced the photostability of $Ag-AgI/Al_2O_3$.

Experimental Section

Chemicals and Materials. The reagent 5,5-dimethyl-1-pyrroline-*N*-oxide (DMPO), used as the spin trapping agent in the ESR studies, was purchased from the Sigma Chemical Co. All other chemicals used were analytical grade, purchased from Beijing Chemical Co. and used without further purification.

Preparation of Catalysts. Mesoporous γ-Al_2O_3 was prepared from precursors of aluminum *i*-propoxide in the presence of glucose in an aqueous system as described previously.[25] AgI was deposited onto Al_2O_3 supports (dark yellow AgI/Al_2O_3) using a deposition−precipitation method described in the Supporting Information. $Ag-AgI/Al_2O_3$ was prepared via a photocatalytic reduction method. A suspension of AgI/Al_2O_3 (0.5 g) in 50 mL of deionized water was sonicated for 30 min. The pH of the suspension was adjusted to 5.97 with a dilute HNO_3 solution. Octadecylamine acetate (0.05 g) was added to the suspension and stirred at 70 °C until the surfactant was dissolved. $AgNO_3$ (7.9 mg) in NH_4OH (0.08 mL, 25 wt % NH_3) was then added to the mixture and stirred in the dark for 30 min. The product was filtered, dried at 100 °C, and calcined in air at 500 °C for 3 h. The catalyst powder was mixed with deionized water and irradiated with visible light ($\lambda > 400$ nm) for 4 h to reduce adsorbed Ag^+ to Ag via AgI photocatalysis. Finally, the product was filtered, rinsed with deionized water, and dried at ambient temperature. The prepared $Ag-AgI/Al_2O_3$ was dark gray. Following this procedure, two different amounts of adsorbed Ag^+ were reduced on the AgI/Al_2O_3 ($Ag1-AgI/Al_2O_3$, $Ag2-AgI/Al_2O_3$). As a reference, Ag/Al_2O_3 was prepared by the incipient wetness impregnation method (Supporting Information).

Characterization. The samples were examined by obtaining XRD patterns (XDS-2000 diffractometer; Scintag Inc., Sunnyvale, CA) and UV−vis diffuse reflectance spectra (Hitachi UV-3100). The X-ray photoelectron spectroscopy (XPS) was taken on an AXIS-Ultra instrument from Kratos using monochromatic Al Kα radiation (225 W, 15 mA, 15 kV) and low-energy electron flooding for charge compensation. Auger electron spectroscopy (AES) was performed on an AXIS-Ultra instrument from Kratos. The BET surface area of various samples was determined by nitrogen adsorption/desorption experiments using a Micromeritics ASAP2000 analyzer (Micromeritics, Norcross, GA). The zeta potential of catalysts in KNO_3 (10^{-3} M) solution were measured with a Zetasizer 2000 (Malvern Co., United Kingdom) with three consistent readings. ESR spectra were obtained using a Bruker model ESP 300 E electron paramagnetic resonance spectrometer equipped with a Quanta-Ray Nd:YAG laser system as the irradiation source (λ = 532 nm). The photocurrent from the various samples was measured in a basic electrochemical system (AMETEK Princeton Applied Research, Oak Ridge, TN) with a two-compartment, three-electrode electrochemical cell equipped with a photocatalyst photoanode (prepared by dip-coating and drying in air at 70 °C) and a platinum wire cathode in a 0.1 M Na_2SO_4 solution. The reference electrode was a saturated calomel electrode.

Photocatalytic Degradation of Chlorophenolic Compounds under Visible Light. Photocatalytic experiments were performed in a beaker with aqueous suspensions of chlorophenol (60 mL, 10 mg L^{-1}) and 100 mg of catalyst powder. The light source was a 350 W Xe-arc lamp (Shanghai Photoelectron Device Ltd.) equipped with wavelength cutoff filters for $\lambda > 420$ and 450 nm and focused onto the beaker. Prior to irradiation, the suspensions were magnetically stirred in the dark for ca. 30 min to establish adsorption/desorption equilibrium between the pollutants and the surface of the catalyst under room air-equilibrated conditions. The concentration of each chlorophenol was measured using high-performance liquid chromatography (1200 series; Agilent) with an Eclipse XDB-C18 column (5 μm, 4.6 × 150 mm; Agilent). The total organic carbon of each solution was measured with an Apollo 9000 TOC analyzer.

Results and Discussion

Characterization of Photocatalysts. Figure 1 shows the XRD patterns of different samples. A mixture of β-AgI and γ-AgI was formed on AgI/Al_2O_3 and $Ag-AgI/Al_2O_3$, while the AgI crystal size became smaller on $Ag-AgI/Al_2O_3$.

In the process of the preparation of $Ag-AgI/Al_2O_3$, first, the supported AgI became amorphous after AgI/Al_2O_3 was calcined in air at 500 °C for 3 h (curve c),[26] and then the mixture of β-AgI and γ-AgI formed again on Al_2O_3 with the reduction of Ag^+ in visible-light-illuminated suspensions, leading to the smaller size. Standard peaks of pure γ-Al_2O_3 can be seen in the diffractograms of the support Al_2O_3, and $Al(OH)_3$ diffraction peaks appear on AgI/Al_2O_3 forming in the deposition−precipitation process. No diffraction peaks of Ag^0 species were

(20) Awazu, K.; Fujimaki, M.; Rockstuhl, C.; Tominaga, J.; Murakami, H.; Ohki, Y.; Yoshida, N.; Watanabe, T. *J. Am. Chem. Soc.* **2008**, *130*, 1676–1680.
(21) Wang, P.; Huang, B.; Qin, X.; Zhang, X.; Dai, Y.; Wei, J.; Whangbo, M. *Angew. Chem., Int. Ed.* **2008**, *47*, 7931–7933.
(22) Hu, C.; Lan, Y.; Qu, J.; Hu, X.; Wang, A. *J. Phys. Chem. B* **2006**, *110*, 4066–4072.
(23) Hu, C.; Hu, X.; Wang, L.; Qu, J.; Wang, A. *Environ. Sci. Technol.* **2006**, *40*, 7903–7907.
(24) Rodrigues, S.; Uma, S.; Martyanov, I. N.; Klabunde, K. J. *J. Catal.* **2005**, *233*, 405–410.
(25) Xu, B.; Xiao, T.; Yan, Z.; Sun, X.; Sloan, J.; González-Cortés, S. L.; Alshahrani, F.; Green, M. L. H. *Microporous Mesoporous Mater.* **2006**, *91*, 293–295.
(26) Uvarov, N. F.; Bokhonov, B. B.; Politov, A. A.; Vaněk, P.; Petzelt, J. *J. Mater. Synth. Process* **2000**, *8*, 327–332.

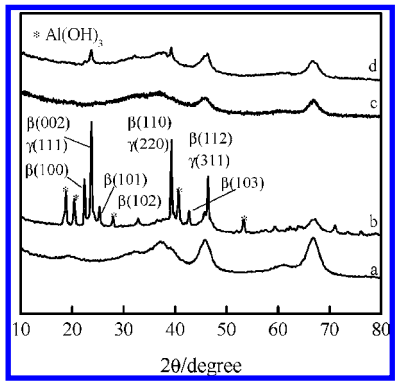

Figure 1. XRD patterns of (a) Al_2O_3, (b) AgI/Al_2O_3, (c) AgI/Al_2O_3 after being calcined at 500 °C, and (d) Ag−AgI/Al_2O_3.

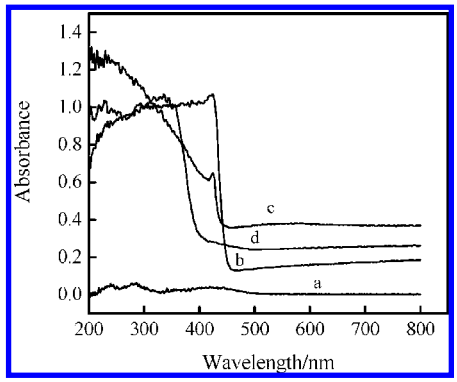

Figure 2. Diffuse reflectance UV−vis spectra of (a) Al_2O_3, (b) AgI/Al_2O_3, (c) Ag−AgI/Al_2O_3, and (d) $TiO_{2-x}N_x$.

observed. This presumably contributed to the incorporation of its low content, small particle size, and high dispersion on the surface of AgI/Al_2O_3. According to the XPS data (XPS sensitivity factor: 4.04), the concentration of the surface silver was 1.55 atom %, whereas that of iodine was 0.6 atom %. The atomic ratio of silver and iodine was about 2.58 more than the stoichiometric ratio of AgI, indicating the existence of Ag^0 species. The metallic state of silver could not be definitely confirmed by XPS and AES measurements due to lower content. However, the Ag^0 species on Ag−AgI/Al_2O_3 could be measured semiquantitatively by UV−vis DRS.[27−29] The optical properties of different samples were shown in Figure 2, including nitrogen-doped TiO_2 ($TiO_{2-x}N_x$), which is considered the standard example of a visible-light photocatalyst prepared as a reference.[30]

The mesoporous Al_2O_3 was transparent at wavelengths between 200 and 800 nm. AgI/Al_2O_3 exhibited a UV absorption band around 200−400 nm and a visible absorption band around 400−430 nm assigned to the light absorption of AgI. In addition to these, Ag−AgI/Al_2O_3 exhibited a band around 400−600 nm assigned to surface plasmon absorption of Ag NPs, indicating the presence of Ag^0 on the surface of Ag−AgI/Al_2O_3. Furthermore, the relative UV−vis absorption spectra of Ag−AgI were difference spectra between those of Ag−AgI/Al_2O_3 and Al_2O_3 (Figure 3). The band at 205 nm was attributed to the highly

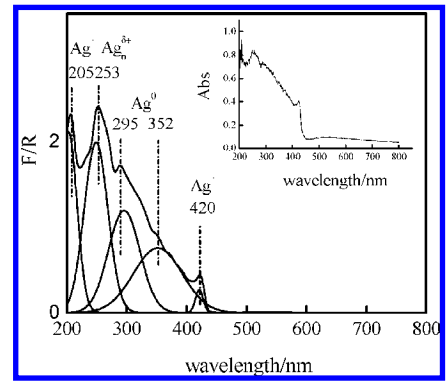

Figure 3. Deconvoluted subbands of Ag−AgI. Inset showing relative diffuse reflectance UV−vis spectra of Ag−AgI.

dispersed Ag^+ ions,[31] 253 nm was assigned to small $Ag_n^{\delta+}$ clusters,[32] and the bands at 295 and 352 nm were attributed to Ag^0 NPs.[33] The other plasmon absorption bands at more than 450 nm were so weak that they were overlaid by the Al_2O_3 baseline, which was observed in the following experiments. Subsequently, the spectra were converted into Kubelka−Munk functions and deconvoluted into Gaussian subbands that could be assigned to different Ag species.[34] The deconvolution was carried out based on the relative intensities of these subbands, and the corresponding percentage of the different Ag species was obtained. Thus, in the tested Ag−AgI/Al_2O_3, the contents of Ag^0 species were about 5.5 wt %. By the same estimation, the contents of Ag^0 species were 6.5, 7.3, and 5.2 wt % for Ag1−AgI/Al_2O_3, Ag2−AgI/Al_2O_3, and Ag/Al_2O_3, respectively. The Ag^0 species were main components on the Ag/Al_2O_3, with absorption bands at 371 and 456 nm (Supporting Information Figure S1). The BET surface areas were 220, 208, 211, and 287 $m^2\ g^{-1}$ for Ag−AgI/Al_2O_3, AgI/Al_2O_3, Ag /Al_2O_3, and Al_2O_3, indicating Ag−AgI have higher dispersion on Al_2O_3.

Photodegradation of Pollutants under Visible-Light Irradiation. To evaluate the plasmon-induced photocatalytic activity of Ag NPs on Ag−AgI/Al_2O_3, the photodegradation of 2-CP was carried out in aqueous dispersions under different visible irradiation after the adsorption of 2-CP onto the Ag−AgI/Al_2O_3 in dark had reached equilibrium (Figure 4). As a comparison, 2-CP degradations were also performed in AgI/Al_2O_3, Ag/Al_2O_3, and $TiO_{2-x}N_x$ suspensions under identical conditions.

In dark within 30 min, the adsorption reached equilibrium, and about 20% of 2-CP were adsorbed onto Ag−AgI/Al_2O_3. Under the same conditions, about 6% and 8% of 2-CP were adsorbed onto AgI/Al_2O_3 and Ag/Al_2O_3. The more adsorptive capacity of Ag−AgI/Al_2O_3 was more possibly contributed to its surface charge properties than their surface area. Most of 2-CP was in its undissociated form at the tested neutral pH values due to its pK_a 8.49. The adsorption of 2-CP was favored at the neutral surface of the catalyst. The pH of point of zero charge (pH_{pzc}) vlues were 5.9, 7.4, and 8.5 for Ag−AgI/Al_2O_3, AgI/Al_2O_3, and Ag/Al_2O_3, respectively (Supporting Information Figure S2). When the pH of aqueous solution is near the pH_{PZC} of the oxide, most of the surface hydroxyl groups are in a neutral state; nearly no surface charge exists. Therefore, the surface of

(27) Shimizu, K.; Tsuzuki, M.; Kato, K.; Yokota, S.; Okumura, K.; Satsuma, A. *J. Phys. Chem. C* **2007**, *111*, 950–959.
(28) Sato, K.; Yoshinari, T.; Kintaichi, Y.; Haneda, M.; Hamada, H. *Appl. Catal., B* **2003**, *44*, 67–78.
(29) She, X.; Flytzani-Stephanopoulos, M. *J. Catal.* **2006**, *237*, 79–93.
(30) Kontos, A. I.; Kontos, A. G.; Raptis, Y. S.; Falaras, P. *Phys. Status Solidi (RRL)* **2008**, *2*, 83–85.
(31) Bogdanchikova, N.; Meunier, F. C.; Avalos-Borja, M.; Breen, J. P.; Pestryakov, A. *Appl. Catal., B* **2002**, *36*, 287–297.
(32) Li, Z.; Stephanopoulos, M. F. *J. Catal.* **1999**, *182*, 313–327.
(33) Shimizu, K.; Shibata, J.; Yoshida, H.; Satsuma, A.; Hattori, T. *Appl. Catal., B* **2001**, *30*, 151–162.
(34) Zhang, L.; Zhang, C.; He, H. *J. Catal.* **2009**, *261*, 101–109.

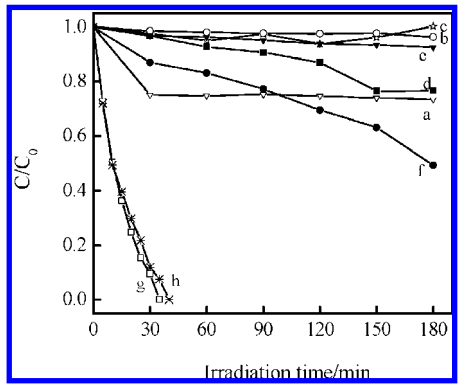

Figure 4. Temporal course of photodegradation of 2-CP (10 mg L^{-1}; 60 mL) in aqueous dispersions (containing catalyst: 1.6 g L^{-1}): (a) Ag−AgI/Al_2O_3 in dark, (b) no catalyst; (d) AgI/Al_2O_3, (e) Ag/Al_2O_3 (f) $TiO_{2-x}N_x$, (g) Ag−AgI/Al_2O_3 with $\lambda > 420$ nm; and (c) AgI/Al_2O_3, (h) Ag−AgI/Al_2O_3 with $\lambda > 450$ nm.

Ag−AgI/Al_2O_3 more tended to the neutral state favoring to adsorb 2-CP at the neutral pH. When irradiated at wavelengths $\lambda > 420$ nm, neither visible light nor Ag/Al_2O_3 showed any activity for the 2-CP degradation, while the rate of 2-CP photodegradation on Ag−AgI/Al_2O_3 was 49 and 22 times faster than that on AgI/Al_2O_3 and $TiO_{2-x}N_x$, respectively. At wavelengths $\lambda > 450$ nm, no significant degradation was observed on AgI/Al_2O_3, which absorbed hardly in these wavelengths range, while Ag−AgI/Al_2O_3 exhibited almost the same photocatalytic activity as it did at $\lambda > 420$ nm. These results indicated that the enhanced degradation of 2-CP was due to the plasmon resonance of Ag NPs rather than the result of electron trapping by Ag NPs and enhanced electron−hole separation, especially with $\lambda > 450$ nm light irradiation. The plasmon-induced activity of Ag NPs was not observed in Ag/Al_2O_3 because no electron transfer occurred from Ag NPs to dielectric Al_2O_3. Therefore, AgI NPs also played an important role in the enhanced activity of Ag−AgI/Al_2O_3. Ag1−AgI/Al_2O_3, Ag2−AgI/Al_2O_3 with 6.5, 7.3 wt % Ag NPs showed slightly lower activity (Supporting Information Figure S3). The results indicated that there was an optimal loading amount of Ag NPs on AgI/Al_2O_3. The excess Ag NPs would lead to its lower dispersion, causing lower activity. In addition, 2,4-dichlorophenol (2,4-DCP) and trichlorophenol (TCP) were completely degraded within 15 and 20 min, respectively, in Ag−AgI/Al_2O_3 suspension under visible-light irradiation (Figure 5A). The percent total organic carbon (TOC) removal was 93%, 81%, and 71% after 120 min for 2-CP, 2,4-DCP, and TCP, respectively (Figure 5B).

Furthermore, under $\lambda > 330$ nm irradiation of the Xe arc lamp, which produces light spectra similar to that of solar radiation, the tested compounds were completely degraded within 5−15 min, and around 90% of the TOC was removed after 60 min. The sequences were different between the degradation of initial compounds and their mineralization due to different oxidation reactions. The former mainly involved dechlorination, while the latter involved further degradation of byproducts. Some byproducts from 2,4-DCP and TCP still contained chlorine groups on the benzene ring, leading to the lower degradation rate. Also, under simulated solar light ($\lambda > 330$ nm), the photoactivity of Ag−AgI/Al_2O_3 was much higher than that of P25 TiO_2 for the degradation of 2-CP (Supporting Information Figure S4). Only with visible-light irradiation, no significant photodegradation of 2-CP was observed in P25 TiO_2 suspension (Supporting Information Figure S5). The photocatalytic activity did not markedly decrease after six successive cycles of degradation testing under visible irradiation (Supporting Information Figure S6). These results indicated that Ag−AgI/Al_2O_3 was an effective and stable plasmon-induced catalyst under solar light.

Reaction Mechanism. In the range of wavelength $\lambda < 450$ nm, both AgI and Ag NPs have light absorption, and the higher activity of Ag−AgI/Al_2O_3 is from photoexcited AgI semiconductor and plasmon-induced Ag NPs. The photocatalytic mechanism of AgI has been elucidated in our previous report.[23] It has been verified that Ag NPs could act as a sinker for photoinduced charge carriers, promoting charge separation to enhance the overall photocatalytic efficiency in contact with semiconductor.[35−37] Herein, the mechanism of Ag NPs plasmon-induced photocatalysis was investigated in detail. First, the effects of various radical scavengers on the degradation of 2-CP were examined under visible-light irradiation.

As shown in Figure 6, the degradation of 2-CP was markedly depressed by HCO_3^-, while it was depressed to some extent by methanol and *t*-butanol in Ag−AgI/Al_2O_3 suspension. HCO_3^- was found to have high adsorption on the surface of the catalyst. The adsorbed HCO_3^- reacted with h^+ and adsorbed $^{\bullet}OH$ on the catalyst, leading to lower activity. Because the $^{\bullet}OH$ scavengers methanol and *t*-butanol hardly adsorbed on the catalyst, they predominantly scavenged $^{\bullet}OH$ in solution. This result indicated that the positive hole (h^+) or the surface-adsorbed $^{\bullet}OH$ was the main reactive oxygen species in the reaction. Meanwhile, with the addition of $O_2^{\bullet-}$ scavenger *p*-benzoquinone, the degradation of 2-CP was also markedly depressed, suggesting the existence of $O_2^{\bullet-}$ in the reaction.

The result was confirmed by the study of ESR with DMPO in Figure 7. The characterization peaks of DMPO-$O_2^{\bullet-}$ were obviously observed in Ag−AgI/Al_2O_3 suspension with visible-light irradiation ($\lambda = 532$ nm). No such signals were detected in dark. Neither AgI/Al_2O_3 nor Ag/Al_2O_3 suspensions showed

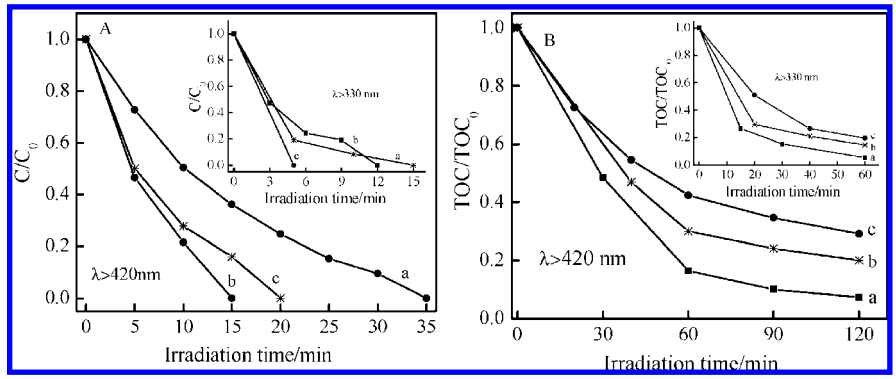

Figure 5. Photodegradation and mineralization of different pollutants (10 mg L^{-1}) in aqueous dispersions of Ag−AgI/Al_2O_3 under visible light $\lambda > 420$ nm and $\lambda > 330$ nm (inset) simulated solar irradiation: (A) C/C_0, (B) TOC/TOC_0. For all panels, (a) 2-CP, (b) 2,4-DCP, and (c) TCP.

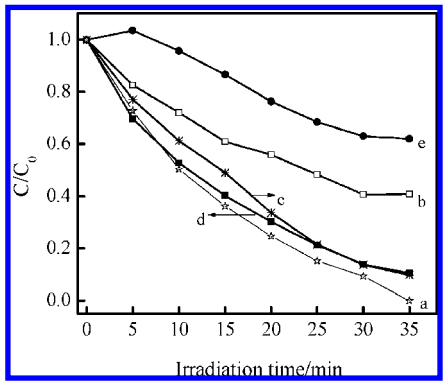

Figure 6. Plotted degradation kinetics of 2-CP in Ag−AgI/Al$_2$O$_3$ suspension (1.6 g L^{-1}) under visible irradiation ($\lambda > 420$ nm) with (a) no scavenger added, (b) 0.1 mM *p*-benzoquinone, (c) *t*-butanol, (d) methanol, and (e) NaHCO$_3$. Scavenger concentration: 0.1 M.

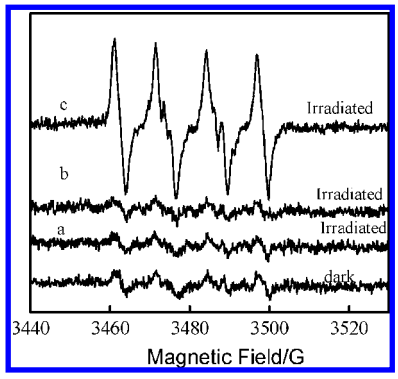

Figure 7. ESR signal of the DMPO-$O_2^{\bullet-}$ in various methanol dispersions under visible-light irradiation (532 nm): (a) Ag/Al$_2$O$_3$, (b) AgI/Al$_2$O$_3$, and (c) Ag−AgI/Al$_2$O$_3$ before and after irradiation.

any signals under the otherwise identical conditions. The reduction potential of the conduction band of AgI is −0.15 V so that the electron in the conduction band (CB) from plasmon-induced Ag NPs could reduce oxygen to $O_2^{\bullet-}$.[38] The photocatalytic oxygen reduction also has been observed at the AgI-covered silver electrode by McMahon etal.[39] The results suggested that $O_2^{\bullet-}$ radicals were generated by the pasmon-induced electron transfer from Ag NPs to the CB of AgI.

Furthermore, the transfer processes of plasmon-induced charges were also followed by CV analysis. In a N$_2$-saturated 0.1 M sodium sulfate aqueous solution (Figure 8A), no significant photocurrent was detected at the Ag−AgI/Al$_2$O$_3$ photoanode in the dark. However, under visible irradiation, the photocurrent increased and then decreased to zero, resulting in a peak, which was contributed to the oxidation of Ag NPs. The intensity of this peak decreased as the illumination wavelength was increased from 420 to 600 nm. With the addition of Fe^{2+} ions to act as electron donors, the peaks gradually decreased and became indiscernible at 5 mM Fe^{2+}, with the consequent formation of a stable photocurrent. Conversely, the oxidation peak did not appear on the AgI/Al$_2$O$_3$ catalyst, and a stable photocurrent was observed only when irradiated between 420 and 450 nm (Figure 8B). This coincides with the window of photocatalytic activity for AgI/Al$_2$O$_3$. The above results indicated that the mechanism of photoinduced charge separation was different in Ag−AgI/Al$_2$O$_3$ and AgI/Al$_2$O$_3$. In the former system, photocurrent generation was ascribed to oxidation of Ag by surface plasmon absorption of Ag NPs, which could then be reduced by Fe^{2+} to obtain photostable Ag NPs and stable photocurrent. The latter catalyst generated a photocurrent from photoexcited AgI as evidenced by the visible-light response. In addition, neither oxidation of Ag nor photocurrent was observed at the Ag/Al$_2$O$_3$ photoanode under the otherwise identical conditions (Supporting Information Figure S7A). It was confirmed that plasmon-induced electron transfer did not occur from Ag NPs to Al$_2$O$_3$. A similar phenomenon was observed in air (Figure 8C) at Ag−AgI/Al$_2$O$_3$. Differently, the oxidation peak of Ag NPs was observed even in the dark due to the presence of oxygen, which showed the strongest intensity. Under visible-light irradiation, oxygen in air mainly trapped the CB electron of AgI from plasmon-induced Ag NPs forming $O_2^{\bullet-}$, and the oxidation of Ag NPs predominantly came from the plasmon-induced charge separation. In the meanwhile, electrons from photoexcited AgI with $\lambda > 420$ nm light could be transferred to Ag NPs[37] to reduce the oxidized silver. Therefore, the oxidation peak of Ag NPs became weaker after light irradiation than before in air. However, Ag NPs were not oxidized at Ag/Al$_2$O$_3$ in air before and after light irradiation due to the passive support (Supporting Information Figure S7B). With the addition of 2-CP, the photocurrent dropped to zero, and the oxidation peak disappeared. This result revealed that 2-CP could be oxidized by plasmon-induced h^+ on Ag NPs, thereby accelerating the photooxidized Ag NPs back to their initial state. This confirmed that plasmon-induced h^+ was one of the primary active species. The consumption of $O_2^{\bullet-}$ generated by the trapping of excited electrons in Ag NPs quenched any photocurrent by the oxidation of 2-CP. Based on all of the information, one electron transfer occurred from the photoexcited Ag NPs to the AgI conduction band, resulting in the formation of $O_2^{\bullet-}$. The other electron transfer occurred from 2-CP to the Ag NPs. Therefore, due to

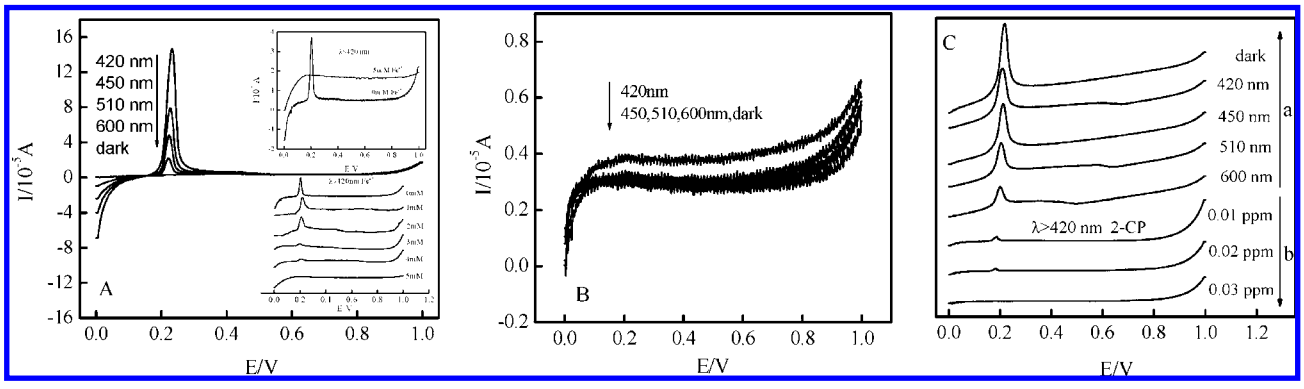

Figure 8. The photocurrent changes at the Ag−AgI/Al$_2$O$_3$ photoanode in N$_2$-saturated (A,B) and air-saturated (C) 0.1 M sodium sulfate aqueous solutions under the specified conditions.

the plasmon-induced charge separation and transfer, Ag NPs were not corrupted by light and resulted in significantly more stable Ag halides. Furthermore, the oxidation of Ag NPs shown in Figure 8A and C indicated that the plasmon-induced charge separation was mainly in $\lambda > 420$ nm visible-light-irradiated Ag−AgI/Al_2O_3 suspension. The higher photoactivity of Ag−AgI/Al_2O_3 possibly contributed to the collective oxidation of $O_2^{\bullet-}$ and excited h^+ on Ag NPs for pollutants.

Conclusions

A plasmonic photocatalyst Ag−AgI/Al_2O_3 was prepared and showed high activity for the degradation and mineralization of 2-CP, 2,4-DCP, and TCP. Two electron transfer processes were observed from the excited Ag NPs to AgI and from 2-CP to the Ag NPs in the photoreaction system by CV analysis. Both $O_2^{\bullet-}$ and excited h^+ on Ag NPs were the main active species in the degradation reaction, having been generated by charge separation and transfer from plasmon-excited Ag NPs. A plasmon-induced mechanism of photocatalysis was proposed. This finding indicates that the high photosensitivity of noble metal NPs could be applied toward the development of new plasmonic visible-light-sensitive photocatalysts and photovoltaic fuel cells.

Acknowledgment. This work was supported by the NSFC (nos. 50921064, 20807051, 20537020), 973 project (no. 2010CB933600), and 863 project (no. 2006AA06Z304).

Supporting Information Available: Preparation procedures for AgI/Al_2O_3 and Ag/Al_2O_3, deconvoluted subbands of Ag/Al_2O_3, the effect of various Ag NPs amount on Ag−AgI/Al_2O_3, isoelectric points of different samples, and the photoactivity comparison of Ag−AgI/Al_2O_3 and P25 TiO_2 under simulated solar, photocurrent generation at Ag/Al_2O_3 photoanode under different conditions. This material is available free of charge via the Internet at http://pubs.acs.org.

JA907792D

(35) Subramanian, V.; Wolf, E. E.; Kamat, P. V. *J. Am. Chem. Soc.* **2004**, *126*, 4943–4950.
(36) Hirakawa, T.; Kamat, P. V. *J. Am. Chem. Soc.* **2005**, *127*, 3928–3934.
(37) Hirakawa, T.; Kamat, P. V. *Langmuir* **2004**, *20*, 5645–5647.
(38) Li, Y.; Zhang, H.; Guo, Z.; Han, J.; Zhao, X.; Zhao, Q.; Kim, S. *Langmuir* **2008**, *24*, 8351–8357.
(39) McMahon, J. J.; Barry, M.; Breen, K. J.; Radziwon, A. K.; Brooks, L. D.; Blair, M. R. *J. Phys. Chem. C* **2008**, *112*, 1158–1166.